New insights into the modulation of ocean biogeochemistry by iron

Alessandro Tagliabue[1*], Andrew Bowie[2], Philip Boyd[2], Kristen Buck[3], Kenneth Johnson[4] and Mak Saito[5]

1. University of Liverpool, United Kingdom
2. Institute for Marine and Antarctic Studies, University of Tasmania, Australia
3. University of South Florida, USA
4. Monterey Bay Aquarium Research Institute, USA
5. Woods Hole Oceanographic Institution, USA

[*]Corresponding author: a.tagliabue@liverpool.ac.uk

Preface

Our understanding of the regulation of the magnitude of global and regional primary productivity has been fundamentally altered with the growing recognition of the pervasive role of iron. Observations of this trace metal in the ocean have increased markedly over recent decades, permitting a new synthesis of the processes governing its oceanic cycle. In particular, the inextricable linkages between iron and wider ocean biogeochemistry, including the cycling of carbon and major nutrients are beginning to emerge.

1. The emergence of the 'Iron Hypothesis'

Ocean primary production is crucial to the Earth System, underpinning the functioning of the global carbon cycle, air-sea CO_2 exchange and marine ecosystems[1]. In the past three decades the micronutrient iron has gone from a relative curiosity to emerging as a key elemental resource that shapes the magnitude and dynamics of primary production in the global ocean. Oceanographers first became interested in iron in the 1930s as an explanation as to why the major nutrient inventories (nitrogen and phosphorus) were not fully depleted by primary producers in surface waters of much of the Southern Ocean[2-4]. Indeed, early laboratory studies showed that iron enrichment stimulated the growth of phytoplankton[5], providing encouragement that iron could control phytoplankton growth in seawater[6,7]. However, due to the low solubility of iron in the modern oxic ocean[8] and the tendency for iron to be 'scavenged' from the water column by sinking particles[9], dissolved iron was likely to be a rare commodity for ocean biota. By the early 1980s the crucial role for iron as a co-factor in many cellular enzymes, particularly those linked with photosynthesis, respiration and nitrogen fixation had been identified[10,11]. Yet despite this body of knowledge, it was not until the early 2000s that the global importance of iron to ocean productivity and biogeochemistry became widely acknowledged and included in global ocean models[12].

A key issue hindering the study of iron-phytoplankton interactions in the ocean was the need for contamination-free sampling and accurate measurements at the required pico to nanomolar levels (10^{-12} to 10^{-9} moles L^{-1}). Only in the late 1970s did development of exacting trace metal clean sampling protocols[13] and an appreciation for the rigours of clean analytical methods[14] allow the first reliable oceanic iron observations, which showed low surface water concentrations and 'nutrient-like' behaviour through the water column[15,16]. Results from shipboard iron enrichment experiments of natural phytoplankton communities conducted with ultra-clean methods resurrected the idea that a lack of iron was indeed a key feature of the Southern Ocean[17,18]. This led John Martin to formulate the '*iron hypothesis*', which proposed that greater delivery of dust iron to the Southern Ocean during glacial periods led to enhanced utilisation of the major nutrients and a corresponding drawdown of atmospheric carbon dioxide[19] (see also Box 1). Subsequent model simulations showed that if the reserves of major nutrients in the Southern Ocean could be exhausted, then atmospheric CO_2 levels could be reduced significantly by 60 to 100 ppm[20]. Martin's provocative ideas about how iron fertilisation might control past and future climate are now oceanographic folklore and have catalysed research into this field.

57   Due to the perceived limitations of Martin's shipboard experiments (e.g. exclusion of grazers)[21],
58   only a deliberate *in situ* iron fertilisation was deemed able to satisfactorily corroborate the *in vitro*
59   evidence of iron-limited phytoplankton growth. These were initially performed during the 1990s in
60   iron-limited equatorial Pacific waters[22,23] and by 2000, results were published from the first test of
61   the iron hypothesis in the Southern Ocean[24]. As of present, more than a dozen mesoscale iron
62   fertilisation experiments have been carried out worldwide, demonstrating phytoplankton iron
63   limitation in the Southern, Equatorial Pacific and subarctic Pacific Oceans[25,26]. Additional shipboard
64   experiments also point to a role for iron limitation in the subpolar North Atlantic Ocean[27], California
65   Current[28] and Humboldt and Peru upwelling systems[29].
66
67   The undeniable role for iron in shaping patterns of ocean productivity necessitated an
68   understanding of the processes that regulate the ocean iron cycle itself. In 1997 an important step
69   was made when Johnson and co-workers[30] compiled 354 internally consistent iron observations
70   and produced a conceptual view of how the ocean iron cycle operated (Fig. 1), which was
71   supported by a one dimensional model that reproduced observed profiles from a number of sites
72   (largely in the Pacific Ocean). This model[30] assumed that (i) iron-rich aeolian dust input was the
73   major external source of iron to the ocean, (ii) deep ocean iron concentrations were held to a
74   quasi-constant value of approximately 0.6 nmol L^{-1} by uniform levels of the recently quantified
75   organic iron-complexing ligands[31,32] that protected dissolved iron from scavenging and (iii) that
76   despite emerging knowledge of substantial variations in the biological iron demand[33], the uptake of
77   iron and its regeneration from sinking organic matter was closely coupled to phosphorus at basin
78   scales. This synthesis effort[30] (Fig 1) ultimately catalysed the full representation of iron cycling with
79   three dimensional ocean general circulation models[34,35]. Subsequent synthesis efforts in the
80   following years[36,37] echoed this general paradigm for the ocean iron cycle, which still informs a
81   large number of global iron models today[38]. Models based on this view of the ocean iron cycle
82   attribute up to half of the 80 ppm glacial decrease in atmospheric carbon dioxide to iron
83   fertilisation[39,40].
84
85   In this Review we will explore how the recent expansion of observational data has challenged the
86   prevailing understanding of the ocean iron cycle. New sources and cycling processes are
87   identified, which requires an overhaul of the way in which the models we rely on for future
88   projections represent this important resource. These insights permit a new synthesis of the main
89   processes involved in the global ocean iron cycle and the important linkages to the cycling of
90   carbon and other nutrients. Ultimately we highlight where future advances may be fruitful in
91   advancing our understanding. If this can be achieved, it would substantially reduce uncertainties in
92   our ability to project the impact of environmental change on the ocean carbon cycle.
93
94   **2. Refining our understanding of the iron cycle and its biogeochemical linkages**
95
96   In recent years there has been a near 100-fold increase in the number of high quality iron
97   measurements available to explore processes and assess global models[41]. Initially, only a few
98   laboratories worldwide had the capability to sample for and measure iron in the ocean, resulting in
99   relatively sparse datasets. In an effort to remedy this, in the early 2000's the international
100   community galvanised around a global project called "GEOTRACES" (www.geotraces.org) that
101   seeks to systematically document the distribution of trace elements and isotopes, including iron,
102   throughout the oceans[42]. Critical in this regard was an earlier intercalibration effort in 2004 called
103   "Sampling and Analysis of Iron" (SAFe) that sought to intercompare a suite of analytical techniques
104   and trace metal clean sampling methodologies from different laboratories at sea[43]. Importantly, it
105   also produced a set of readily available 'reference samples' with consensus values at
106   oceanographically relevant concentrations that could be used by both new and established
107   investigators to evaluate their analytical methods. GEOTRACES has since launched a number of
108   interwoven basin-scale "sectional" studies, complemented by prior targeted process studies to
109   understand temporal iron dynamics[44] and the drivers of "naturally fertilised" regions in the wake of
110   Southern Ocean island systems[45,46]. Thanks to these multi-faceted efforts, there are more than
111   20,000 available observations of iron from the ocean at present. This expansion in our ability to
112   observe the system has allowed our understanding of how the ocean iron cycle operates to be
113   refined.

114
115 **2.1 Recognition of external sources and cycling of iron**
116
117 A key finding from both the GEOTRACES programme and studies of process studies of natural
118 systems was the recognition that there are multiple external sources of iron to the ocean that are
119 significant at both regional and global scales. For example, studies of enhanced biological activity
120 downstream of Southern Ocean island systems[45,46] and offshore from continental margins[47], the
121 ability to track the origins of offshore iron pools via its mineral make up[48] and parallel modelling
122 experiments[49] have emphasised that iron supply from continental margins extends far beyond the
123 coastal zone. Equally, GEOTRACES efforts in the Atlantic[50], Pacific[51], Southern[52] and Arctic[53]
124 Oceans have observed striking signals of iron associated with hydrothermal activity along mid
125 ocean ridges that make a key contribution to the deep ocean iron inventory[49,54]. Due to their
126 important role in the high latitude regions of the ocean crucial for air-sea CO_2 exchange,
127 continental margin and hydrothermal sources play a dominant role in shaping the global carbon
128 cycle[49]. However, the role for dust may have been enhanced during glacial periods typified by
129 greater Southern Ocean dust fluxes.
130
131 While the perceived role for dust in regulating the functioning of the ocean carbon cycle via its
132 modulation of high latitude ocean productivity has diminished in recent years, it remains a key
133 supply mechanism to the low latitude ocean. This is illustrated by new high precision iron isotope
134 studies that have, via the distinct isotopic signal associated with crustal iron, quantified the
135 contribution of dust to dissolved iron in the tropical Atlantic Ocean[55]. The productivity of this region
136 is typically limited by nitrogen[56] and when enough iron is supplied it permits the growth of nitrogen-
137 fixing organisms[57]. More broadly speaking, iron supply has emerged as a major driving force
138 behind the geographic extent and magnitude of nitrogen fixation in the tropics[58-60]. Dust-driven
139 changes in iron supply to the low latitude ocean has therefore emerged as an important
140 component of the maintenance of the oceanic fixed nitrogen inventory[61].
141
142 An important hypothesis from the initial view of the ocean iron cycle was the concept of the
143 buffering of dissolved iron to a constant deep-water concentration by uniform concentrations of
144 organic iron-complexing ligands. However, a parallel expansion of ligand observations over recent
145 decades[62,63], including basin scale ocean sections[64,65], reveals that their abundance varies from
146 less than 1 to more than 2 nmol L^{-1} even in the ocean interior. Potential ligand sources associated
147 with iron-limited bacterial and phytoplankton community growth, zooplankton grazing and particle
148 breakdown have emerged[62], as well as potential external inputs associated with dust[66] or
149 rainwater[67] and the microbial production of strong iron-binding siderophores[68]. There is also the
150 likelihood that subduction and equatorward transport of excess ligands from high latitudes can
151 remotely influence the interior distribution of dissolved iron[69]. As they control the residence time of
152 iron in the ocean[70], the cycling of organic iron-complexing ligands has also emerged as a crucial
153 component of the ocean iron cycle. For instance, modelling indicates that variations in ligand
154 concentration have a larger influence on contemporary atmospheric carbon dioxide levels than
155 dust iron supply[49] and can be responsible for long range transport of iron away from point sources
156 (e.g. hydrothermal vents)[51].
157
158 **2.2 Biological Iron Cycling**
159
160 The phytoplankton demand for iron relative to carbon or phosphorus (i.e. their 'stoichiometry') is a
161 common way of evaluating the coupling between the biological cycling of different resources.
162 Despite its initial representation in numerical and conceptual models (Fig 1) as a constant
163 quantity[30,35], it is now well established that phytoplankton can exhibit substantial variations in their
164 iron stoichiometry between different environments[33,71]. For example, phytoplankton from the low
165 iron waters of the Southern Ocean typically exhibit cellular demands that are more than five-fold
166 lower than those from the iron rich tropical Atlantic[71,72]. This level of stoichiometric plasticity
167 extends far beyond that seen for the major nutrients[73] and is crucial in linking the biological cycling
168 of iron to the assimilation of major nutrients and carbon fixation. Another unique feature for iron is
169 the key role for iron regeneration by zooplankton, bacteria and viruses in supporting iron supply to
170 the biota[74]. A number of process studies have documented regional and seasonal variation in the

3

171 importance of regenerated iron in fuelling phytoplankton carbon fixation[74,75] and a potentially
172 important role for higher trophic levels organisms is also emerging[76]. Lastly, specific characteristics
173 associated with remineralisation of particulate iron, relative to major nutrients[77] can decouple the
174 vertical profile of dissolved iron in the ocean from other nutrients[78].
175
176 How iron affects rates of carbon and nitrogen fixation is fundamentally linked to the process of iron
177 acquisition by the biota. Early studies demonstrated that only the dissolved iron not bound to iron
178 complexing organic ligands was bioavailable[6,79]. While the sum of these 'free' inorganic species
179 may indeed be the most bioavailable form of iron[80], its concentration in seawater is vanishingly low
180 ($<10^{-15}$ moles L^{-1}). More recently, laboratory[81] and field[82] experiments have demonstrated that
181 phytoplankton are also able to access the more dominant organically complexed iron pool via high
182 affinity acquisition systems, such as ferric reductases and this strategy appears to be prevalent in
183 the iron-poor Southern Ocean[81]. In the dust dominated low latitude regions of the Atlantic Ocean
184 the nitrogen fixing cyanobacterium *Trichodesmium* has been shown to directly access mineral
185 particulate iron[83]. Taken together, this highlights a range of iron acquisition strategies that may be
186 differentially linked to the commonly measured 'dissolved' iron concentration.
187
188 When detailed process studies combine measurements of ocean physics, major nutrient
189 distributions and inputs with biological activity the intricate links between the cycling of iron and
190 other nutrients and carbon can be illuminated. Across the tropical Atlantic Ocean it has been
191 demonstrated that synoptic variation in dust input, linked to variations in the Inter Tropical
192 Convergence Zone, controls the 'biogeochemical divide' between phosphorus and iron limitation of
193 nitrogen fixing plankton[59]. In the Pacific Ocean, metaproteomic techniques find gradual transitions
194 from nitrogen to iron stress between the subtropical Pacific Gyre and the Equatorial Pacific that are
195 linked to the underlying physics, with continuing iron stress in the south Pacific Gyre[84]. These
196 approaches provide basin-scale perspectives on how the distinct environmental characteristics of
197 different ocean biomes translate into gradients in the resource regulation of biological activity.
198
199 **2.3 A new synthesis of the ocean iron cycle and its wider connections**
200
201 Bringing together these new insights allows an updated synthesis of how the ocean iron cycle
202 operates and its connections with the cycles of carbon and nitrogen (Fig 2). In doing so, we are
203 required to make a broad distinction between the dominance of dust iron at low latitudes and the
204 greater role for sedimentary and hydrothermal iron sources at high latitudes. While iron supply at
205 the high latitudes drives the connections to the wider oceanic cycling of carbon and air-sea carbon
206 dioxide exchanges, low latitude dust supply contributes to the maintenance of the fixed nitrogen
207 inventory of the ocean. The drivers of the interior distribution of iron are more complicated than for
208 major nutrients (see Box 1), with roles played by deep ocean iron sources, the independent
209 regeneration of iron from sinking particles and scavenging, as well as by the remote influence of
210 water masses subducted from high latitudes and transported equatorward. Previously, close
211 linkages between the cycling of iron and major nutrients such as phosphorus were emphasised
212 (Fig 1). However, as discussed above, multiple unique factors for iron have now been identified,
213 exemplified by the substantial decoupling between observations of phosphate and iron along a
214 meridional section in the West Atlantic Ocean[85] (Fig 3).
215
216 Synthesising these new insights provides a more refined picture of the ocean iron cycle and
217 emphasises key meridional contrasts (Fig 2). At high latitudes, upwelling and mixing of iron into
218 surface waters is the major supply mechanism fuelling biological activity that is sustained via iron
219 recycling by zooplankton and bacteria. Due to longer remineralisation length scales, iron export to
220 the ocean interior is more efficient than for major nutrients (phosphorus is emphasised in Fig 2)
221 and decouples subsurface iron reserves from those of major nutrients[78]. As high latitudes are often
222 iron limited, ligand production by iron stressed communities and depletion of dissolved iron stocks
223 leaves an excess of iron-complexing ligands that can be subducted and transported equatorward
224 (dashed arrows in Fig 2). In contrast, low latitudes are strongly affected by dust and the associated
225 iron supply fuels nitrogen fixation by *Trichodesmium, Crocosphera* and other diazotrophs. Dust
226 may act as a source or sink for iron both in the surface ocean and during its sedimentation into the
227 ocean interior. For example, in the iron replete Mediterranean, dust deposition actually depleted

228 dissolved iron levels due to the enhanced particle scavenging[86]. In low latitude regions where dust
229 supply is low and upwelling absent, the ensuing iron stress leads to low rates of nitrogen fixation[87].
230 Subsurface iron at low latitudes will be affected by the balance between local iron regeneration
231 from sinking organic material and scavenging onto lithogenic and organic particles[88]. As
232 scavenging rates are closely linked to the amount of iron not organically complexed, subsurface
233 iron in the low latitudes can also be remotely controlled by subduction and equatorward transport
234 of high latitude waters with excess ligands[69].

236 This integrated view of the ocean iron cycle places additional challenges on the global ocean
237 models we rely on for testing hypotheses and projections of change. For example, those global
238 models that more closely track the developments in our understanding of the ocean iron cycle
239 encapsulated in Fig 2 are better able to reproduce observed features emerging from the iron data
240 collected along large GEOTRACES ocean sections[38]. When models reflect the existence of
241 multiple iron sources and unique aspects to iron's oceanic cycling, simulated glacial iron
242 fertilisation contributes less than a quarter to decrease in the glacial carbon dioxide (despite
243 enhancing Southern Ocean biological activity)[89]. At present, inter-model differences result in iron
244 residence times that range widely, from a few years to a few hundred years[38]. This uncertainty
245 regarding the representation of iron in global models is important as projections of how climate
246 change will affect ocean productivity[90], which has implications for global carbon cycling and marine
247 ecosystems, will be regulated by iron over large swathes of the upper ocean. Reducing uncertainty
248 requires that we are able to dig deeper into the new oceanic survey data to extract quantitative
249 information on the rates and controlling factors of the mechanisms governing the ocean iron cycle
250 to inform accurate model parameterisations.

252 **3. Linking iron to the cycles of carbon and other nutrients: new challenges and**
253 **opportunities**

255 The rapid increase in iron observations over recent decades has led to a much clearer
256 understanding of the myriad processes underpinning the ocean iron cycle and its connections to
257 the cycling of carbon and major nutrients (Fig 2). However, a complete theoretical framework for
258 how iron cycling embeds within the broader context of ocean biogeochemical cycling is still lacking,
259 which limits our ability to project future trends with confidence[38]. The expanding coverage of ocean
260 observations via the GEOTRACES surveys[41] is essential, but alone is insufficient to constrain the
261 key underlying processes.

263 **3.1 Physical linkages across different space and time scales**

265 The new proliferation of full depth, basin scale ocean sections for iron have been instrumental in
266 advancing our understanding of the ocean iron cycle (Fig 2). However, the 'biogeochemical'
267 processes of interest (e.g. iron regeneration, scavenging, ligand production) operate on the
268 backdrop of different physical processes that must be taken into consideration to extract
269 information on the underlying biogeochemical processes (see Box 1). For instance, a given
270 oceanic section is overlain with signatures of different water masses reflecting their individual end
271 member conditions, interior flow pathways and transit times, which confound interpretation of iron
272 distributions. That said, observed features in iron distributions can themselves be 'fingerprinted'
273 using conservative tracers (either steady state or transient) of specific iron sources and cycling
274 pathways.

276 Water masses leave the ocean surface via the process of subduction and are transported along
277 lines of constant potential vorticity in the ocean interior[91]. Therefore, water masses provide a
278 framework for the deeper examination of biogeochemical properties. For example, on the recent
279 zonal GA03 GEOTRACES section in the North Atlantic Ocean, an Optimum Multi Parameter
280 Analysis was undertaken whereby the hydrographic and major nutrient data was used to
281 objectively identify nine primary watermasses[92]. Such a physical framework permits the evaluation
282 of how water masses originating from different locations, with specific iron characteristics (e.g. low
283 iron water from the high latitudes and high iron Mediterranean water) affect the distribution of iron
284 throughout the basin. The vertical distributions of iron at a given location should be evaluated in its

285 proper physical context (i.e. in density space), to account for the physical variability that often
286 complicates interpretations based on absolute depths[78].
287
288 Steady state and transient tracers provide an excellent opportunity to fingerprint specific iron
289 sources and assess iron input fluxes or regeneration and scavenging rates. Volcanic helium-3 has
290 been used to identify iron plumes associated with mid ocean ridges[50,51,54], as well as derive large
291 scale hydrothermal fluxes when estimates of global helium efflux are combined with the slope of
292 the iron versus helium relationship[51]. The radium decay series, which is used to quantify
293 exchanges at ocean boundaries, is also measured on some GEOTRACES sections[93] and may be
294 linked to dissolved iron datasets to estimate a range of iron boundary fluxes. A particularly
295 promising avenue may be the combination of such tracers with iron isotope studies. Tracers of
296 ocean ventilation, such as chlorofluorocarbons or tritium, and diagnostics of interior ocean flows,
297 such as potential vorticity, can be used to provide a coherent context within which to quantify how
298 iron concentrations are modified, e.g. by regeneration or scavenging, during the transit of a water
299 parcel subducted from the ocean surface (see: Box 1, Fig 4a) or away from a specific point source
300 (e.g. a mid ocean ridge or continental margin). As shown in Fig 3, phosphate distributions are
301 almost always closely linked to lines of constant potential vorticity following the major physical
302 flows, whereas the distributions of iron have little obvious connection, highlighting distinctions
303 between the cycling of these two nutrients.
304
305 Ultimately we require a robust means to isolate the different contributors to the iron cycle within a
306 holistic physical framework (Box 1, Figure 4a), as exists for major nutrients. This would allow the
307 global significance of ocean physics, regeneration and scavenging to iron distributions to be jointly
308 elucidated[69]. With this approach, the first order levels of coupling and decoupling between iron and
309 major nutrients like phosphate may be quantified for use in parameterising the foundations of
310 global models. Furthermore, considering iron observations within their physical context, e.g. water
311 masses, density or potential vorticity, will facilitate the quantification of the rates of key processes.
312 Exploiting the coherent iron-hydrography datasets from GEOTRACES and targeted process
313 studies is needed to achieve this goal.
314
315 **3.2 Which iron pools underpin variations in iron cycling?**
316
317 While the new synthesis (Fig 2) expands our understanding of how iron links to wider
318 biogeochemical cycling, the underlying processes themselves are ultimately governed by the
319 particular functional forms of iron that define its 'reactivity'. It is important to consider reactivity in
320 different ways depending on particular process. Biological reactivity (or bioavailability) affects the
321 ability of the biota to acquire iron or how bacteria remineralise iron from organic material, while
322 chemical reactivity will modulate the dissolution of lithogenic iron and the propensity of different
323 forms of iron to be transferred to particulate pools via scavenging or colloidal aggregation. A key
324 contrast between iron and the major nutrients is that while specific chemical forms of nitrogen (e.g.
325 nitrate) or phosphorus (e.g. phosphate) are measured, iron measurements rely on operational
326 definitions. The prime focus of ocean iron observations remains on separating 'dissolved' and
327 particulate iron, i.e. all forms of iron that pass through (or are retained by) a defined filter (normally
328 0.2 μm). However, somewhere between half and three quarters of dissolved iron does not pass a
329 smaller 0.02 μm filter, which has led to a further distinction between 'soluble' and 'colloidal'
330 dissolved iron[94].
331
332 Until relatively recently, most of the focus on the iron present in these different size fractions has
333 been from a geochemical or chemical perspective on inorganic species - emphasising the degree
334 of complexation between iron and ligands in soluble and colloidal pools[94] or the solubility and
335 mineralogy of colloidal and particulate iron[95]. However, due to the scarcity and bio-essential nature
336 of iron, much of the iron reservoir must be associated with the biota and their biochemical
337 components. For instance, phytoplankton and bacteria are a notable fraction of the small
338 particulate iron pool[96], while the virus-associated iron may be a non-negligible component of
339 colloidal iron[97]. Additionally, intracellular iron, that is largely associated with metalloenzymes and
340 storage proteins[98] will be released to the dissolved phase following microbial grazing and viral lysis
341 of biogenic particles. Notable examples of biomolecules that may contribute to the dissolved or

342 colloidal iron pool when released from cells include numerous metalloenzymes and their iron-
343 binding constituents (e.g. hemes and iron-sulphur clusters)[99], as well as ferritin and bacteroferritin
344 (iron storage proteins)[98]. While the magnitude of their contribution to measured iron levels and their
345 lifetime in the dissolved phase remain unknown, these biogenic iron species will contribute to the
346 biological and chemical reactivity of iron in different environments. On-going work with new ultra
347 high mass resolution mass spectrometry and 'omics based studies are delving deeper into the
348 'black box' of what makes up different iron pools, which will be crucial in better understanding the
349 biological and/or chemical reactivity of iron. A key challenge in this regard is the transient nature of
350 these different components of the ocean iron pool, which is affected by the specific attributes of
351 distinct environments and will ultimately regulate the linkages between iron and other
352 biogeochemical cycles (Fig 4b).
353
354 **3.3. Transcending the scale window: New frontiers for the ocean iron cycle**
355
356 Will we see the same step change in our understanding of the ocean iron cycle over the next
357 decade? The importance of iron in regulating ocean productivity and biogeochemical cycling is well
358 established and as we have discussed, important aspects unique to its oceanic cycling, relative to
359 major nutrients, have been identified (Figs 2 and 3). Thus to be able to project the impacts of
360 ocean change with confidence, iron needs to be fully integrated into a theoretical framework where
361 the main drivers of its distribution and cycling are identified, as for major nutrients. This would
362 enable progress to be made in the representation of iron cycling in the ocean models we rely on to
363 test hypotheses and appraise the consequences of on-going climate change. Enormous progress
364 has been made in our ability to observe ocean iron distributions thanks to GEOTRACES, but better
365 understanding of the roles played by different biological, chemical and physical processes remains
366 elusive. In part this is due to our fragmentary picture of ocean iron cycle variability and the linkages
367 to global biogeochemical cycles.
368
369 When iron measurements are conducted at similar scales to other biogeochemical tracers during
370 targeted experiments, budgets and fluxes can be quantified, which yield insight into the linkages
371 that ultimately regulate the functioning of the ocean's biogeochemical cycles. For example, the
372 FeCycle experiment followed iron dynamics in a labelled patch of the subantarctic Southern
373 Ocean, documenting the parallel roles of ocean physics, biology and chemistry in governing links
374 between iron and broader aspects of biogeochemical cycling, including dust iron supply[44]. Two
375 multi-disciplinary experiments focussing on the naturally fertilised Kerguelen plateau region in
376 different seasons were able to develop regional iron budgets[75] and make wider links to physical
377 and biological processes, including downward biogenic carbon export and air-sea CO_2 exchange.
378 We recommend future work that expands such efforts to the ocean basin scale, coupling ocean
379 sections with insights into the associated physical, chemical, biochemical and ecological
380 processes. This may be achieved in its simplest sense by expanding the biological, biochemical
381 and physical measurements conducted on GEOTRACES sections, as for the GA03 north Atlantic
382 section[72,92]. More ambitiously, key regions along sections (e.g. downstream of iron sources or
383 across gradients of iron stress) may be targeted and controlled volume experiments performed to
384 elucidate the governing processes. Finally, expanding the temporal scale of iron sampling requires
385 advances in analytical chemistry, which may ultimately yield the autonomous sensors or remote
386 samplers for iron needed to transform our ability to observe variability (e.g. at time-series stations).
387 For instance, this could illuminate how natural climate variations (e.g. El Nino in the Pacific) or
388 seasonal transitions (e.g. at high latitudes or in coastal upwellings) shape biogeochemical cycles
389 via modifications to iron dynamics.
390

Figure Legends

Figure 1. A schematic representation of the first view of the processes governing the ocean iron cycle. The major external source is dust, with the iron supplied from continental margins and hydrothermal activity on mid ocean ridges thought to be lost from the dissolved pool close to the source. Release of iron from dust or supply from upwelling stimulates biological activity, nitrogen fixation and particulate organic matter fluxes in a constant relationship to major nutrients. In the ocean interior, iron regeneration and scavenging is controlled by fixed concentrations of iron binding organic ligands.

Figure 2. A revised representation of the major processes in the ocean iron cycle. A broad meridional contrast is emphasised between the iron-limited Southern Ocean and the major nutrient limited low latitude regimes. Dust remains dominant in the low latitudes, but continental margin and upwelled hydrothermal sources are more important in the Southern Ocean. Flexible iron uptake and biological cycling, along with the production of excess iron binding ligands dominate the Southern Ocean, whereas nitrogen fixation occurs in the low latitudes (although this process can also be restricted by lack of iron outside of the north Atlantic subtropical gyre). The particulate organic iron flux is decoupled from that of phosphorus at high latitudes and the flux of lithogenic material is important at low latitudes influenced by dust. Subduction of excess organic iron binding ligands from the Southern Ocean has a remote influence on the interior ocean at low latitudes.

Figure 3. Dissolved phosphate (upper panel) and dissolved iron (lower panel) observations collected along the GA02 GEOTRACES meridional section in the west Atlantic[85] as a function of latitude, with contours of constant potential vorticity overlain.

Figure 4. a) A schematic representation of how iron cycle processes can be placed within a holistic physical framework. Subduction of a water mass between density layers (σ_1 and σ_2) and subsequent spreading along lines of constant potential vorticity transports iron signals. This remote impact will then affect the interpretation of observed local phenomena. The terminology of the iron and ligand pools is described in Box 1. b) An illustration of the different components of particulate and dissolved iron (including the soluble and colloidal components Emphasis is on a fluid continuum of soluble, colloidal and particulate iron, as well as the role of inorganic (bottom half: nano particles and lithogenic species) and organic components (top half: encompassing biogenic and biomolecules that bind iron strongly, as well as weaker diffuse iron-binding ligands such as hemes, saccharides or fulvic acids).

Box 1: Using theory to identify first order governing processes

A suite of interleaving processes controls the distributions of nutrients in the ocean. Biological uptake and chemical removal constitute sinks, whereas external inputs and regeneration are sources. Physical transport also transfers nutrients between surface and deep waters and throughout the ocean interior. Thus, interior ocean phosphate (P_{TOT}) is the sum of preformed (physically transported into the ocean interior, P_{PRE}) and regenerated (i.e. from sinking organic matter, P_{REG}) pools:

$$P_{TOT} = P_{PRE} + P_{REG} \quad (1)$$

P_{REG} is quantified using apparent oxygen utilisation (AOU) and the phosphate:oxygen ratio ($R_{P:O2}$):

$$P_{REG} = R_{P:O2} AOU \quad (2)$$

Equations 1 and 2 then quantify the varying influences of ocean circulation and biological activity on phosphorus cycling[100,101]. As the biological pump shifts phosphorus from the preformed to the regenerated pool, P_{REG}/P_{TOT} (known as P^*) quantifies the efficiency of the biological pump[100]. Observations indicate that the biological pump operates at around one-third efficiency, with a linear relationship between P^* and atmospheric CO_2 levels[100]. This theory underpins the '*iron hypothesis*'[19], whereby additional iron enhances the biological pump efficiency by shifting extra phosphate from the preformed to the regenerated pool and lowering CO_2.

While a similar theory for iron (Fe_{TOT}) would include preformed (Fe_{PRE}) and regenerated (Fe_{REG}) components, it must also consider subsurface sediment (Fe_{SED}) and hydrothermal (Fe_{HYD}) input, alongside iron scavenging loss (Fe_{SCAV}). The dust iron deposited within the mixed layer affects Fe_{PRE}, but the smaller amount of dust that dissolves in the ocean interior (Fe_{DUST}) must be included:

$$Fe_{TOT} = Fe_{PRE} + Fe_{REG} + Fe_{SED} + Fe_{HYD} + Fe_{DUST} - Fe_{SCAV} \quad (3)$$

Variability in the iron content of sinking organic matter[71] causes a variable $R_{Fe:O2}$ that must be combined with AOU to derive Fe_{REG}. Using Equation 3 within a model finds that Fe_{PRE} interacts with interior sources to shape the magnitude of surface iron supply[69] (Fig 2). Importantly, the regeneration and scavenging balance (i.e. Fe_{REG}-Fe_{SCAV}) is decoupled from the gross rates of regeneration inferred from AOU because upstream subduction of excess ligands places an upper limit on how regeneration impacts total iron[69]. This explains why the slope of the dissolved iron to AOU relationship differs from phytoplankton iron contents[72]. While AOU itself may not be the ideal tracer of remineralisation rates, it offers a tractable means for its basin scale quantification.

If Equation 3 were linked to observations, the first order drivers of the ocean iron cycle could be identified. This can be achieved if estimates of phytoplankton iron content[72,77] are allied to ocean tracers (Sec 3.1). For instance, linking subduction timescales determined from transient tracers to density-based or potential vorticity flow pathways can track preformed iron and its modification. Source-specific tracers, such as helium or radium may isolate hydrothermal and sediment pools. Interior dissolution of dust may be traced via lithogenic tracers such as aluminium and titanium. Finally, other particle reactive elements that are not biologically active (e.g. thorium) can constrain scavenging.

Ultimately, the role of the each term in Equation 3 is affected by organic iron-binding ligands[69] that are usually in excess of iron[63]. A parallel approach for the total ligand concentration (L_{TOT}) should account for preformed surface produced ligands (L_{PRE}), interior ligand production from both organic matter degradation (L_{REG}) or specific sources (L_{SOURCE}), and ligand loss (L_{LOSS}) from bacterial decay and coagulation:

$$L_{TOT} = L_{PRE} + L_{REG} + L_{SOURCE} - L_{LOSS} \quad (4)$$

484 Equation 4 may be quantified by combining experimental studies and tracers, but an important and
485 confounding issue is the diversity of ligands present (i.e. a blend of iron binding molecules typically
486 represented as distinct 'classes' based on measured binding constants), since each may have a
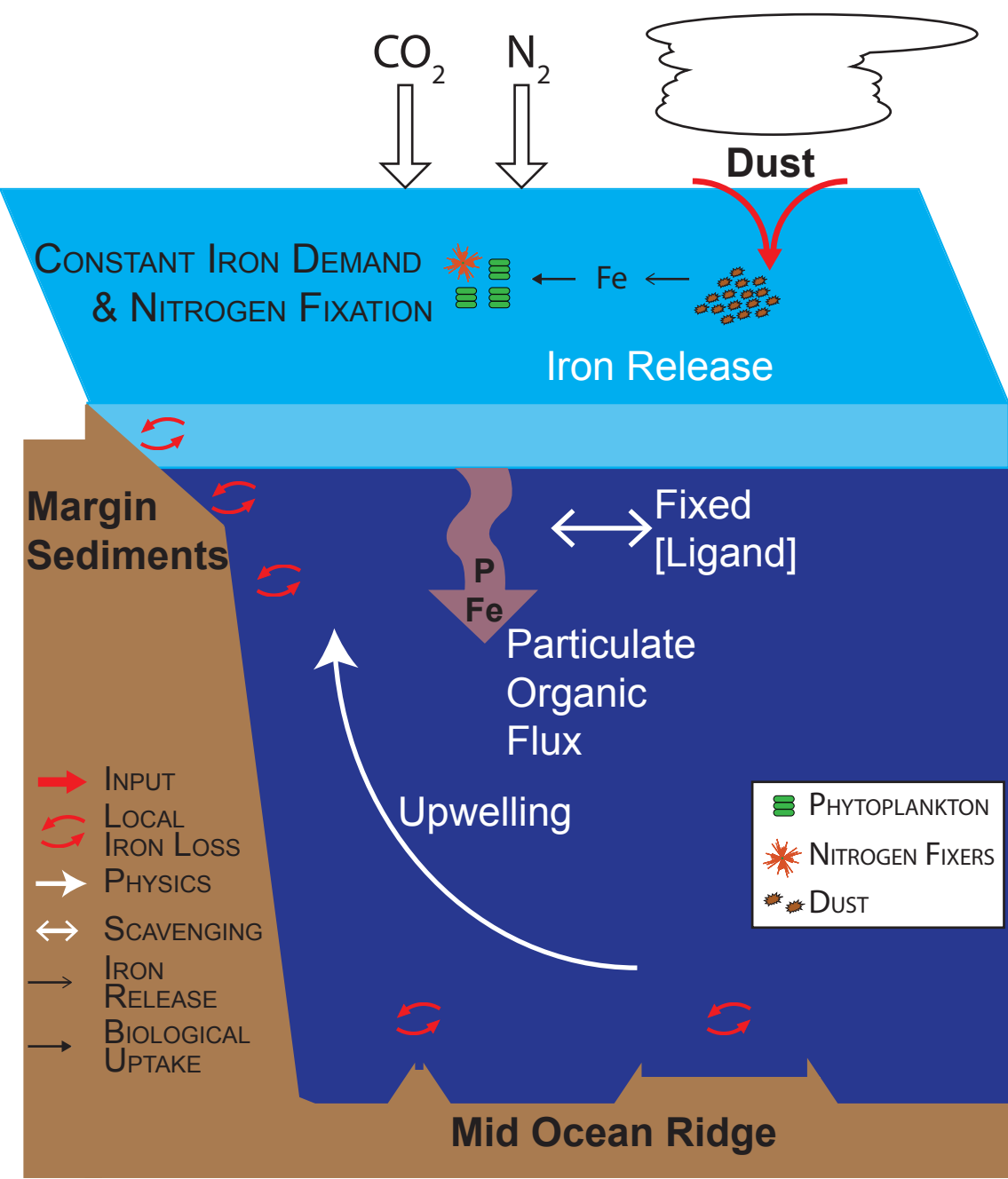487 unique provenance and impact(s) on the iron cycle[62-64].
488

References

1   Falkowski, P. & Raven, J. A. *Aquatic Photosynthesis.* 488 (Princeton University Press, 2007).
2   Ruud, J. T. Nitrates and phosphates in the Southern Seas. *Journal du Conseil* **5**, 347-360 (1930).
3   Gran, H. H. On the conditions for the production of plankton in the sea. *Conseil Perm. Internat. pour l'Explor. de la Mer. Rapp. et Proces-Verb.* **75**, 37-46 (1931).
4   Hart, T. On the phytoplankton of the south-west Atlantic and the Bellingshausen Sea, 1929-31. *Discovery Reports* **VIII**, 1-268 (1934).
5   Harvey, H. On the rate of diatom growth. *Journ. Mar. Biol. Assoc* **19**, 253-276 (1933).
6   Anderson, M. A. & Morel, F. M. M. The influence of aqueous iron chemistry on the uptake of iron by the coastal diatomThalassiosira weissflogii1. *Limnology and Oceanography* **27**, 789-813, doi:10.4319/lo.1982.27.5.0789 (1982).
7   Brand, L. E., Sunda, W. G. & Guillard, R. R. L. Limitation of marine phytoplankton reproductive rates by zinc, manganese and iron. *Limnology and Oceanography* **28**, 1182-1198, doi:10.4319/lo.1983.28.6.1182 (1983).
8   Cooper, L. H. N. Iron in the Sea and in Marine Plankton. *Proceedings of the Royal Society B: Biological Sciences* **118**, 419-438, doi:10.1098/rspb.1935.0064 (1935).
9   Goldberg, E. D. Marine Geochemistry 1. Chemical Scavengers of the Sea. *The Journal of Geology* **62**, 249-265, doi:10.1086/626161 (1954).
10 Williams, R. J. P. The Bakerian Lecture, 1981 - Natural-Selection of the Chemical-Elements. *Proc R Soc Ser B-Bio* **213**, 361-397, doi:10.1098/rspb.1981.0071 (1981).
11 Raven, J. A. The iron and molybdenum use efficiencies of plant growth with different energy, carbon and nitrogen sources. *New Phytologist* **109**, 279-287, doi:10.1111/j.1469-8137.1988.tb04196.x (1988).
12 Moore, J. K., Doney, S. C., Glover, D. M. & Fung, I. Y. Iron cycling and nutrient-limitation patterns in surface waters of the World Ocean. *Deep-Sea Res Pt Ii* **49**, 463-507, doi:10.1016/S0967-0645(01)00109-6 (2002).
13 Bruland, K. W., Franks, R. P., Knauer, G. A. & Martin, J. H. Sampling and analytical methods for the determination of copper, cadmium, zinc, and nickel at the nanogram per liter level in sea water. *Analytica chimica acta* **105**, 233-245, doi:10.1016/s0003-2670(01)83754-5 (1979).
14 Settle, D. & Patterson, C. Lead in albacore: guide to lead pollution in Americans. *Science* **207**, 1167-1176, doi:10.1126/science.6986654 (1980).
15 Gordon, R. M., Martin, J. H. & Knauer, G. A. Iron in Northeast Pacific Waters. *Nature* **299**, 611-612, doi:10.1038/299611a0 (1982).
16 Landing, W. M. & Bruland, K. W. The contrasting biogeochemistry of iron and manganese in the Pacific Ocean. *Geochimica et Cosmochimica Acta* **51**, 29-43, doi:10.1016/0016-7037(87)90004-4 (1987).
17 Martin, J. H., Gordon, R. M. & Fitzwater, S. E. Iron in Antarctic Waters. *Nature* **345**, 156-158, doi:10.1038/345156a0 (1990).
18 Martin, J. H., Fitzwater, S. E. & Gordon, R. M. Iron deficiency limits phytoplankton growth in Antarctic waters. *Global Biogeochemical Cycles* **4**, 5-12, doi:10.1029/GB004i001p00005 (1990).
19 Martin, J. H. Glacial-Interglacial Co2 Change: The Iron Hypothesis. *Paleoceanography* **5**, 1-13, doi:10.1029/Pa005i001p00001 (1990).
20 Joos, F., Sarmiento, J. L. & Siegenthaler, U. Estimates of the effect of Southern Ocean iron fertilization on atmospheric CO2 concentrations. *Nature* **349**, 772-775, doi:10.1038/349772a0 (1991).
21 Cullen, J. J. Hypotheses to explain high-nutrient conditions in the open sea. *Limnology and Oceanography* **36**, 1578-1599, doi:10.4319/lo.1991.36.8.1578 (1991).
22 Martin, J. H. *et al.* Testing the Iron Hypothesis in Ecosystems of the Equatorial Pacific-Ocean. *Nature* **371**, 123-129, doi:10.1038/371123a0 (1994).
23 Coale, K. H. *et al.* A massive phytoplankton bloom induced by an ecosystem-scale iron fertilization experiment in the equatorial Pacific Ocean. *Nature* **383**, 495-501, doi:10.1038/383495a0 (1996).
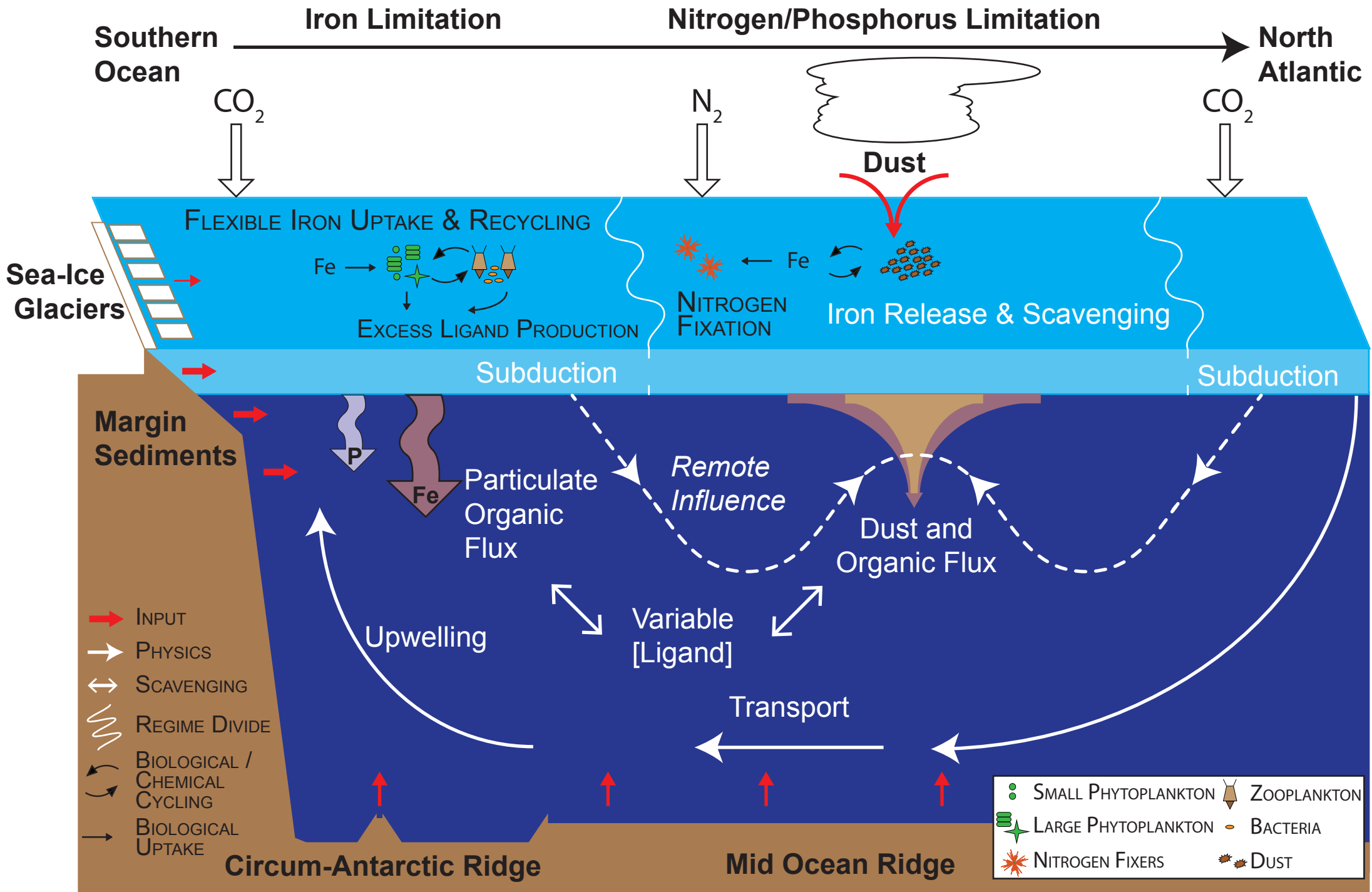
546 24   Boyd, P. W. *et al.* A mesoscale phytoplankton bloom in the polar Southern Ocean
547   stimulated by iron fertilization. *Nature* **407**, 695-702, doi:10.1038/35037500 (2000).
548 25   Boyd, P. W. *et al.* Mesoscale iron enrichment experiments 1993-2005: Synthesis and future
549   directions. *Science* **315**, 612-617, doi:10.1126/Science.1131669 (2007).
550 26   de Baar, H. J. W. *et al.* Synthesis of iron fertilization experiments: From the Iron Age in the
551   Age of Enlightenment. *Journal of Geophysical Research* **110**, doi:10.1029/2004jc002601
552   (2005).
553 27   Moore, C. M. *et al.* Iron limits primary productivity during spring bloom development in the
554   central North Atlantic. *Global Change Biology* **12**, 626-634, doi:10.1111/j.1365-
555   2486.2006.01122.x (2006).
556 28   Hutchins, D. A., DiTullio, G. R., Zhang, Y. & Bruland, K. W. An iron limitation mosaic in the
557   California upwelling regime. *Limnology and Oceanography* **43**, 1037-1054,
558   doi:10.4319/lo.1998.43.6.1037 (1998).
559 29   Hutchins, D. A. *et al.* Phytoplankton iron limitation in the Humboldt Current and Peru
560   Upwelling. *Limnology and Oceanography* **47**, 997-1011, doi:10.4319/lo.2002.47.4.0997
561   (2002).
562 30   Johnson, K. S., Gordon, R. M. & Coale, K. H. What controls dissolved iron concentrations
563   in the world ocean? *Marine Chemistry* **57**, 137-161, doi:10.1016/s0304-4203(97)00043-1
564   (1997).
565 31   Gledhill, M. & van den Berg, C. M. G. Determination of complexation of iron(III) with natural
566   organic complexing ligands in seawater using cathodic stripping voltammetry. *Marine
567   Chemistry* **47**, 41-54, doi:10.1016/0304-4203(94)90012-4 (1994).
568 32   Rue, E. L. & Bruland, K. W. Complexation of iron(III) by natural organic ligands in the
569   Central North Pacific as determined by a new competitive ligand equilibration/adsorptive
570   cathodic stripping voltammetric method. *Marine Chemistry* **50**, 117-138, doi:10.1016/0304-
571   4203(95)00031-I (1995).
572 33   Sunda, W. G. & Huntsman, S. A. Interrelated influence of iron, light and cell size on marine
573   phytoplankton growth. *Nature* **390**, 389-392, doi:10.1038/37093 (1997).
574 34   Archer, D. E. & Johnson, K. A model of the iron cycle in the ocean. *Global Biogeochemical
575   Cycles* **14**, 269-279, doi:10.1029/1999gb900053 (2000).
576 35   Parekh, P., Follows, M. J. & Boyle, E. A. Decoupling of iron and phosphate in the global
577   ocean. *Global Biogeochemical Cycles* **19**, doi:10.1029/2004gb002280 (2005).
578 36   Jickells, T. D. *et al.* Global iron connections between desert dust, ocean biogeochemistry,
579   and climate. *Science* **308**, 67-71, doi:10.1126/Science.1105959 (2005).
580 37   de Baar, H. J. & de Jong, J. T. in *The biogeochemistry of iron in seawater* Vol. 7 (eds D. R.
581   Turner & K. A. Hunter) 123-254 (2001).
582 38   Tagliabue, A. *et al.* How well do global ocean biogeochemistry models simulate dissolved
583   iron distributions? *Global Biogeochemical Cycles*, doi:10.1002/2015gb005289 (2016).
584 39   Hain, M. P., Sigman, D. M. & Haug, G. H. Carbon dioxide effects of Antarctic stratification,
585   North Atlantic Intermediate Water formation, and subantarctic nutrient drawdown during the
586   last ice age: Diagnosis and synthesis in a geochemical box model. *Global Biogeochemical
587   Cycles* **24**, doi:10.1029/2010gb003790 (2010).
588 40   Watson, A. J., Bakker, D. C. E., Ridgwell, A. J., Boyd, P. W. & Law, C. S. Effect of iron
589   supply on Southern Ocean CO2 uptake and implications for glacial atmospheric CO2.
590   *Nature* **407**, 730-733, doi:10.1038/35037561 (2000).
591 41   Mawji, E. *et al.* The GEOTRACES Intermediate Data Product 2014. *Marine Chemistry* **177**,
592   1-8, doi:10.1016/j.marchem.2015.04.005 (2015).
593 42   Anderson, R. & Henderson, G. GEOTRACES—A Global Study of the Marine
594   Biogeochemical Cycles of Trace Elements and Their Isotopes. *Oceanography* **18**, 76-79,
595   doi:10.5670/oceanog.2005.31 (2005).
596 43   Johnson, K. S. *et al.* Developing Standards for Dissolved Iron in Seawater. *Eos,
597   Transactions American Geophysical Union* **88**, 131, doi:10.1029/2007eo110003 (2007).
598 44   Boyd, P. W. *et al.* FeCycle: Attempting an iron biogeochemical budget from a mesoscale
599   SF6 tracer experiment in unperturbed low iron waters. *Global Biogeochemical Cycles* **19**,
600   doi:10.1029/2005gb002494 (2005).
601 45   Blain, S. *et al.* Effect of natural iron fertilization on carbon sequestration in the Southern
602   Ocean. *Nature* **446**, 1070-U1071, doi:10.1038/Nature05700 (2007).
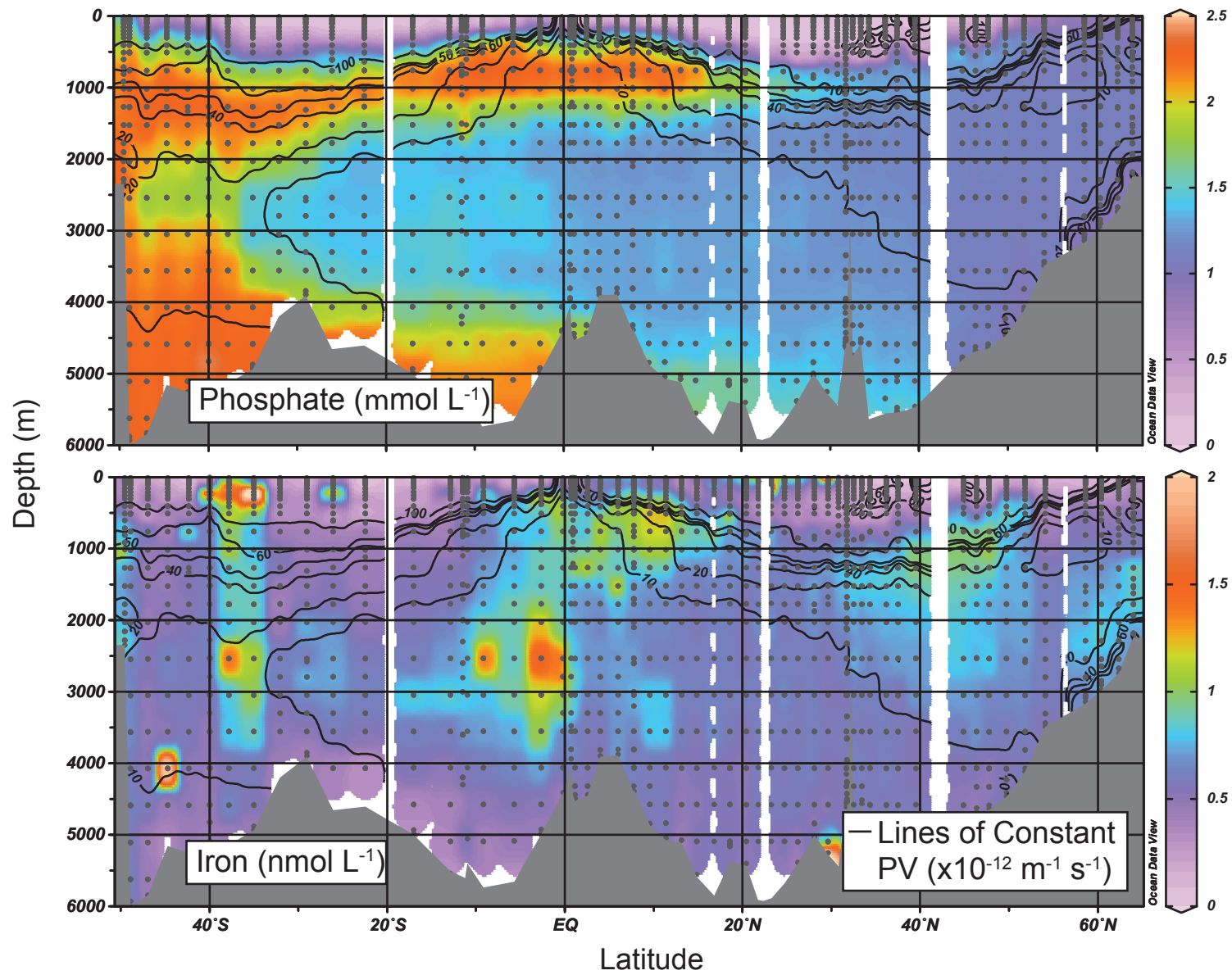
603 46   Pollard, R. T. *et al.* Southern Ocean deep-water carbon export enhanced by natural iron
604   fertilization. *Nature* **457**, 577-580, doi:10.1038/nature07716 (2009).
605 47   Elrod, V. A., Berelson, W. M., Coale, K. H. & Johnson, K. S. The flux of iron from
606   continental shelf sediments: A missing source for global budgets. *Geophysical Research*
607   *Letters* **31**, doi:10.1029/2004gl020216 (2004).
608 48   Lam, P. J. & Bishop, J. K. B. The continental margin is a key source of iron to the HNLC
609   North Pacific Ocean. *Geophysical Research Letters* **35**, doi:10.1029/2008gl033294 (2008).
610 49   Tagliabue, A., Aumont, O. & Bopp, L. The impact of different external sources of iron on the
611   global carbon cycle. *Geophysical Research Letters* **41**, 920-926,
612   doi:10.1002/2013gl059059 (2014).
613 50   Saito, M. A. *et al.* Slow-spreading submarine ridges in the South Atlantic as a significant
614   oceanic iron source. *Nature Geoscience* **6**, 775-779, doi:10.1038/Ngeo1893 (2013).
615 51   Resing, J. A. *et al.* Basin-scale transport of hydrothermal dissolved metals across the South
616   Pacific Ocean. *Nature* **523**, 200-203, doi:10.1038/nature14577 (2015).
617 52   Klunder, M. B., Laan, P., Middag, R., De Baar, H. J. W. & van Ooijen, J. C. Dissolved iron
618   in the Southern Ocean (Atlantic sector). *Deep Sea Research Part II: Topical Studies in*
619   *Oceanography* **58**, 2678-2694, doi:10.1016/j.dsr2.2010.10.042 (2011).
620 53   Klunder, M. B. *et al.* Dissolved iron in the Arctic shelf seas and surface waters of the central
621   Arctic Ocean: Impact of Arctic river water and ice-melt. *J Geophys Res-Oceans* **117**,
622   doi:10.1029/2011jc007133 (2012).
623 54   Tagliabue, A. *et al.* Hydrothermal contribution to the oceanic dissolved iron inventory.
624   *Nature Geoscience* **3**, 252-256, doi:10.1038/ngeo818 (2010).
625 55   Conway, T. M. & John, S. G. Quantification of dissolved iron sources to the North Atlantic
626   Ocean. *Nature* **511**, 212-215, doi:10.1038/nature13482 (2014).
627 56   Moore, C. M. *et al.* Processes and patterns of oceanic nutrient limitation. *Nature*
628   *Geoscience*, doi:10.1038/ngeo1765 (2013).
629 57   Falkowski, P. G. Evolution of the nitrogen cycle and its influence on the biological
630   sequestration of CO2 in the ocean. *Nature* **387**, 272-275, doi:10.1038/387272a0 (1997).
631 58   Moore, C. M. *et al.* Large-scale distribution of Atlantic nitrogen fixation controlled by iron
632   availability. *Nature Geoscience* **2**, 867-871, doi:10.1038/ngeo667 (2009).
633 59   Schlosser, C. *et al.* Seasonal ITCZ migration dynamically controls the location of the
634   (sub)tropical Atlantic biogeochemical divide. *Proceedings of the National Academy of*
635   *Sciences of the United States of America* **111**, 1438-1442, doi:10.1073/pnas.1318670111
636   (2014).
637 60   Dutkiewicz, S., Ward, B. A., Monteiro, F. & Follows, M. J. Interconnection of nitrogen fixers
638   and iron in the Pacific Ocean: Theory and numerical simulations. *Global Biogeochemical*
639   *Cycles* **26**, doi:10.1029/2011gb004039 (2012).
640 61   Weber, T. & Deutsch, C. Local versus basin-scale limitation of marine nitrogen fixation.
641   *Proceedings of the National Academy of Sciences of the United States of America* **111**,
642   8741-8746, doi:10.1073/pnas.1317193111 (2014).
643 62   Gledhill, M. & Buck, K. N. The organic complexation of iron in the marine environment: a
644   review. *Frontiers in microbiology* **3**, 69, doi:10.3389/fmicb.2012.00069 (2012).
645 63   Boyd, P. W. & Tagliabue, A. Using the L* concept to explore controls on the relationship
646   between paired ligand and dissolved iron concentrations in the ocean. *Marine Chemistry*
647   **173**, 52-66, doi:10.1016/j.marchem.2014.12.003 (2015).
648 64   Buck, K. N., Sohst, B. & Sedwick, P. N. The organic complexation of dissolved iron along
649   the U.S. GEOTRACES (GA03) North Atlantic Section. *Deep Sea Research Part II: Topical*
650   *Studies in Oceanography* **116**, 152-165, doi:10.1016/j.dsr2.2014.11.016 (2015).
651 65   Gerringa, L. J. A., Rijkenberg, M. J. A., Schoemann, V., Laan, P. & de Baar, H. J. W.
652   Organic complexation of iron in the West Atlantic Ocean. *Marine Chemistry* **177**, 434-446,
653   doi:10.1016/j.marchem.2015.04.007 (2015).
654 66   Wozniak, A. S., Shelley, R. U., McElhenie, S. D., Landing, W. M. & Hatcher, P. G. Aerosol
655   water soluble organic matter characteristics over the North Atlantic Ocean: Implications for
656   iron-binding ligands and iron solubility. *Marine Chemistry* **173**, 162-172,
657   doi:10.1016/j.marchem.2014.11.002 (2015).
658 67   Cheize, M. *et al.* Iron organic speciation determination in rainwater using cathodic stripping
659   voltammetry. *Analytica chimica acta* **736**, 45-54, doi:10.1016/j.aca.2012.05.011 (2012).

660   68   Mawji, E. *et al.* Production of siderophore type chelates in Atlantic Ocean waters enriched
661   with different carbon and nitrogen sources. *Marine Chemistry* **124**, 90-99,
662   doi:10.1016/j.marchem.2010.12.005 (2011).
663   69   Tagliabue, A., Williams, R. G., Rogan, N., Achterberg, E. P. & Boyd, P. W. A ventilation-
664   based framework to explain the regeneration-scavenging balance of iron in the ocean.
665   *Geophysical Research Letters* **41**, 7227-7236, doi:10.1002/2014gl061066 (2014).
666   70   Völker, C. & Tagliabue, A. Modeling organic iron-binding ligands in a three-dimensional
667   biogeochemical ocean model. *Marine Chemistry* **173**, 67-77,
668   doi:10.1016/j.marchem.2014.11.008 (2015).
669   71   Twining, B. S. & Baines, S. B. The trace metal composition of marine phytoplankton.
670   *Annual review of marine science* **5**, 191-215, doi:10.1146/annurev-marine-121211-172322
671   (2013).
672   72   Twining, B. S., Rauschenberg, S., Morton, P. L. & Vogt, S. Metal contents of phytoplankton
673   and labile particulate material in the North Atlantic Ocean. *Progress in Oceanography* **137**,
674   261-283, doi:10.1016/j.pocean.2015.07.001 (2015).
675   73   Martiny, A. C. *et al.* Strong latitudinal patterns in the elemental ratios of marine plankton
676   and organic matter. *Nature Geoscience* **6**, 279-283, doi:10.1038/ngeo1757 (2013).
677   74   Boyd, P. W. *et al.* Why are biotic iron pools uniform across high- and low-iron pelagic
678   ecosystems? *Global Biogeochemical Cycles* **29**, 1028-1043, doi:10.1002/2014gb005014
679   (2015).
680   75   Bowie, A. R. *et al.* Iron budgets for three distinct biogeochemical sites around the
681   Kerguelen Archipelago (Southern Ocean) during the natural fertilisation study, KEOPS-2.
682   *Biogeosciences* **12**, 4421-4445, doi:10.5194/bg-12-4421-2015 (2015).
683   76   Ratnarajah, L., Bowie, A. R., Lannuzel, D., Meiners, K. M. & Nicol, S. The biogeochemical
684   role of baleen whales and krill in Southern Ocean nutrient cycling. *Plos One* **9**, e114067,
685   doi:10.1371/journal.pone.0114067 (2014).
686   77   Twining, B. S. *et al.* Differential remineralization of major and trace elements in sinking
687   diatoms. *Limnol. Oceanogr* **59**, 689-704, doi:10.4319/lo.2014.59.3.0689 (2014).
688   78   Tagliabue, A. *et al.* Surface-water iron supplies in the Southern Ocean sustained by deep
689   winter mixing. *Nature Geoscience* **7**, 314-320, doi:10.1038/ngeo2101 (2014).
690   79   Hudson, R. J. M. & Morel, F. M. M. Iron transport in marine phytoplankton: Kinetics of
691   cellular and medium coordination reactions. *Limnology and Oceanography* **35**, 1002-1020,
692   doi:10.4319/lo.1990.35.5.1002 (1990).
693   80   Morel, F. M. M., Kustka, A. B. & Shaked, Y. The role of unchelated Fe in the iron nutrition of
694   phytoplankton. *Limnology and Oceanography* **53**, 400-404, doi:10.4319/lo.2008.53.1.0400
695   (2008).
696   81   Strzepek, R. F., Maldonado, M. T., Hunter, K. A., Frew, R. D. & Boyd, P. W. Adaptive
697   strategies by Southern Ocean phytoplankton to lessen iron limitation: Uptake of organically
698   complexed iron and reduced cellular iron requirements. *Limnology and Oceanography* **56**,
699   1983-2002, doi:10.4319/lo.2011.56.6.1983 (2011).
700   82   Maldonado, M. T. & Price, N. M. Utilization of iron bound to strong organic ligands by
701   plankton communities in the subarctic Pacific Ocean. *Deep Sea Research Part II: Topical
702   Studies in Oceanography* **46**, 2447-2473, doi:10.1016/s0967-0645(99)00071-5 (1999).
703   83   Rubin, M., Berman-Frank, I. & Shaked, Y. Dust- and mineral-iron utilization by the marine
704   dinitrogen-fixer Trichodesmium. *Nature Geoscience* **4**, 529-534, doi:10.1038/ngeo1181
705   (2011).
706   84   Saito, M. A. *et al.* Multiple nutrient stresses at intersecting Pacific Ocean biomes detected
707   by protein biomarkers. *Science* **345**, 1173-1177, doi:10.1126/science.1256450 (2014).
708   85   Rijkenberg, M. J. *et al.* The distribution of dissolved iron in the West Atlantic Ocean. *Plos
709   One* **9**, e101323, doi:10.1371/journal.pone.0101323 (2014).
710   86   Wagener, T., Guieu, C. & Leblond, N. Effects of dust deposition on iron cycle in the surface
711   Mediterranean Sea: results from a mesocosm seeding experiment. *Biogeosciences* **7**,
712   3769-3781, doi:Doi 10.5194/Bg-7-3769-2010 (2010).
713   87   Sohm, J. A. *et al.* Nitrogen fixation in the South Atlantic Gyre and the Benguela Upwelling
714   System. *Geophysical Research Letters* **38**, doi:10.1029/2011gl048315 (2011).
715   88   Boyd, P. W. & Ellwood, M. J. The biogeochemical cycle of iron in the ocean. *Nature
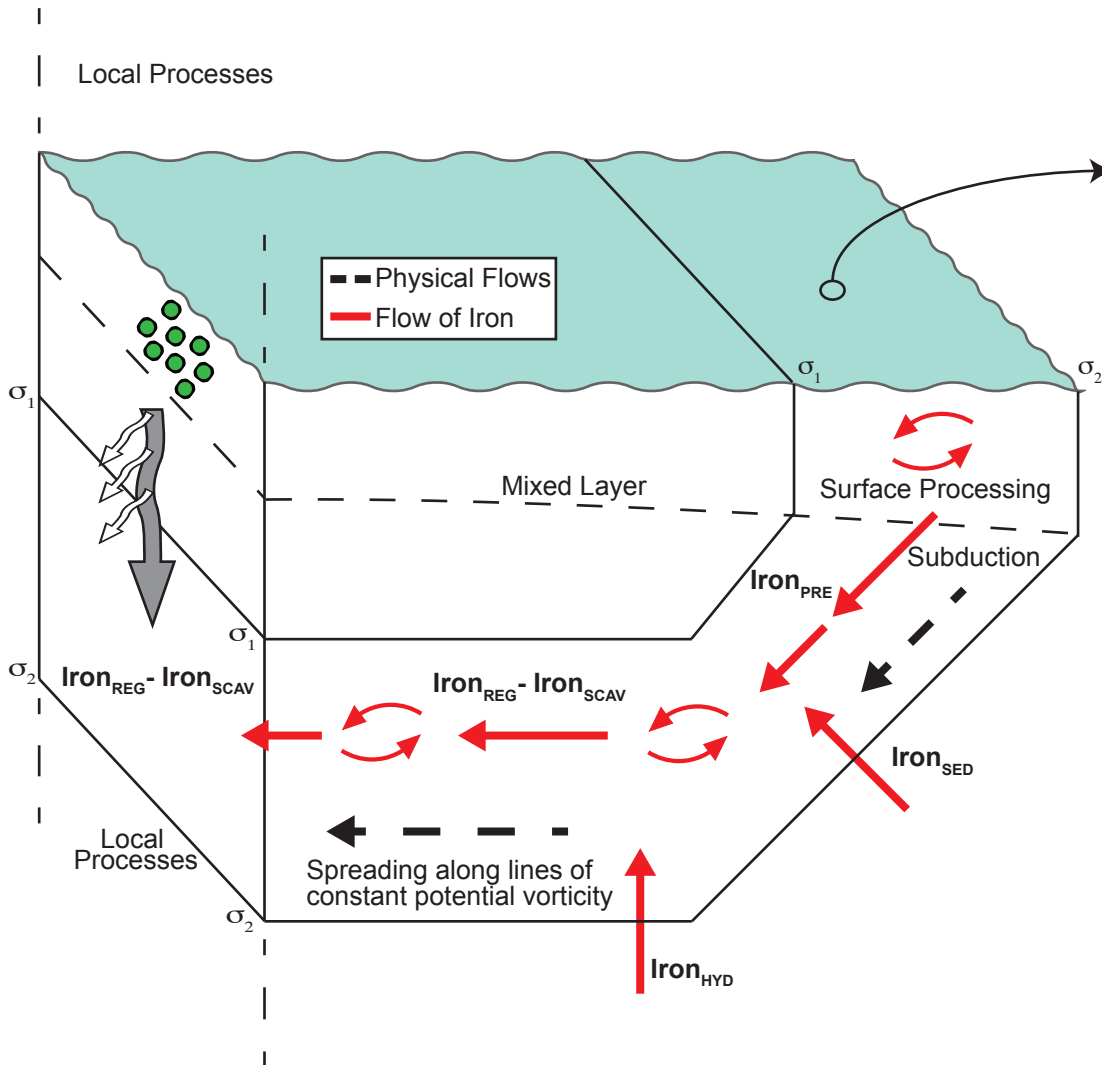716   Geoscience* **3**, 675-682, doi:10.1038/ngeo964 (2010).

717   89   Lambert, F. *et al.* Dust fluxes and iron fertilization in Holocene and Last Glacial Maximum
718   climates. *Geophysical Research Letters* **42**, 6014-6023, doi:10.1002/2015gl064250 (2015).
719   90   Bopp, L. *et al.* Multiple stressors of ocean ecosystems in the 21st century: projections with
720   CMIP5 models. *Biogeosciences* **10**, 6225-6245, doi:10.5194/bg-10-6225-2013 (2013).
721   91   Keffer, T. The Ventilation of the World's Oceans: Maps of the Potential vorticity Field.
722   *Journal of Physical Oceanography* **15**, 509-523, doi:10.1175/1520-
723   0485(1985)015<0509:tvotwo>2.0.co;2 (1985).
724   92   Jenkins, W. J., Smethie, W. M., Boyle, E. A. & Cutter, G. A. Water mass analysis for the
725   U.S. GEOTRACES (GA03) North Atlantic sections. *Deep Sea Research Part II: Topical
726   Studies in Oceanography* **116**, 6-20, doi:10.1016/j.dsr2.2014.11.018 (2015).
727   93   Charette, M. A., Morris, P. J., Henderson, P. B. & Moore, W. S. Radium isotope
728   distributions during the US GEOTRACES North Atlantic cruises. *Marine Chemistry* **177**,
729   184-195, doi:10.1016/j.marchem.2015.01.001 (2015).
730   94   Wu, J., Boyle, E., Sunda, W. & Wen, L. S. Soluble and colloidal iron in the oligotrophic
731   North Atlantic and North Pacific. *Science* **293**, 847-849, doi:10.1126/science.1059251
732   (2001).
733   95   von der Heyden, B. P., Roychoudhury, A. N., Mtshali, T. N., Tyliszczak, T. & Myneni, S. C.
734   Chemically and geographically distinct solid-phase iron pools in the Southern Ocean.
735   *Science* **338**, 1199-1201, doi:10.1126/science.1227504 (2012).
736   96   Tortell, P. D., Maldonado, M. T. & Price, N. M. The role of heterotrophic bacteria in iron-
737   limited ocean ecosystems. *Nature* **383**, 330-332, doi:Doi 10.1038/383330a0 (1996).
738   97   Bonnain, C., Breitbart, M. & Buck, K. N. The Ferrojan Horse Hypothesis: Iron-Virus
739   Interactions in the Ocean. *Frontiers in Marine Science* **3**, doi:10.3389/fmars.2016.00082
740   (2016).
741   98   Mackey, K. R. *et al.* Divergent responses of Atlantic coastal and oceanic Synechococcus to
742   iron limitation. *Proceedings of the National Academy of Sciences of the United States of
743   America* **112**, 9944-9949, doi:10.1073/pnas.1509448112 (2015).
744   99   Hogle, S. L., Barbeau, K. A. & Gledhill, M. Heme in the marine environment: from cells to
745   the iron cycle. *Metallomics* **6**, 1107-1120, doi:10.1039/c4mt00031e (2014).
746   100   Ito, T. & Follows, M. J. Preformed phosphate, soft tissue pump and atmospheric CO2.
747   *Journal of Marine Research* **63**, 813-839, doi:10.1357/0022240054663231 (2005).
748   101   Broecker, W. S., Takahashi, T. & Takahashi, T. Sources and flow patterns of deep-ocean
749   waters as deduced from potential temperature, salinity, and initial phosphate concentration.
750   *Journal of Geophysical Research* **90**, 6925, doi:10.1029/JC090iC04p06925 (1985).
751

CO_2

N_2

Dust

Constant Iron Demand & Nitrogen Fixation

Fe

Iron Release

Margin Sediments

Fixed [Ligand]

P
Fe

Particulate Organic Flux

Upwelling

Input

Local Iron Loss

Physics

Scavenging

Iron Release

Biological Uptake

Phytoplankton

Nitrogen Fixers

Dust

Mid Ocean Ridge

Phosphate (mmol L^{-1})

Iron (nmol L^{-1})

— Lines of Constant
PV (x10^{-12} m^{-1} s^{-1})

Depth (m)

Latitude

Ocean Data View

a) Physical Linkages in the Iron Cycle

Local Processes

σ_1
σ_2

Iron$_{REG}$- Iron$_{SCAV}$

Local Processes

Mixed Layer

Surface Processing

Subduction

Iron$_{PRE}$

Iron$_{REG}$- Iron$_{SCAV}$

Iron$_{SED}$

Spreading along lines of constant potential vorticity

Iron$_{HYD}$

- - - Physical Flows
— Flow of Iron

b) What makes up the different iron pools?

Organic

Inorganic

Iron Storage Proteins

Iron-Sulphur Clusters

Metallo-enzymes

Large Biogenic Iron

Sidero-phores

Diffuse Weak Ligands

Viruses

Detritus

Dissolved Iron

Bacteria

Soluble

Colloidal

Particulate

Free iron

Fine lithogenic particles

Large Nanoparticles

Small Nanoparticles

Large lithogenic particles

Transfer between size fractions

Cycling within a size fraction